

Accepted Manuscript

Synthesis, characterization, cellular uptake and apoptosis-inducing properties of two highly cytotoxic cyclometalated ruthenium(II) β -carboline complexes

Jincan Chen, Fa Peng, Yao Zhang, Baojun Li, Ji She, Xinming Jie, Zhilin Zou, Man Chen, Lanmei Chen



PII: S0223-5234(17)30689-X

DOI: [10.1016/j.ejmech.2017.09.007](https://doi.org/10.1016/j.ejmech.2017.09.007)

Reference: EJMECH 9722

To appear in: *European Journal of Medicinal Chemistry*

Received Date: 12 July 2017

Revised Date: 26 August 2017

Accepted Date: 4 September 2017

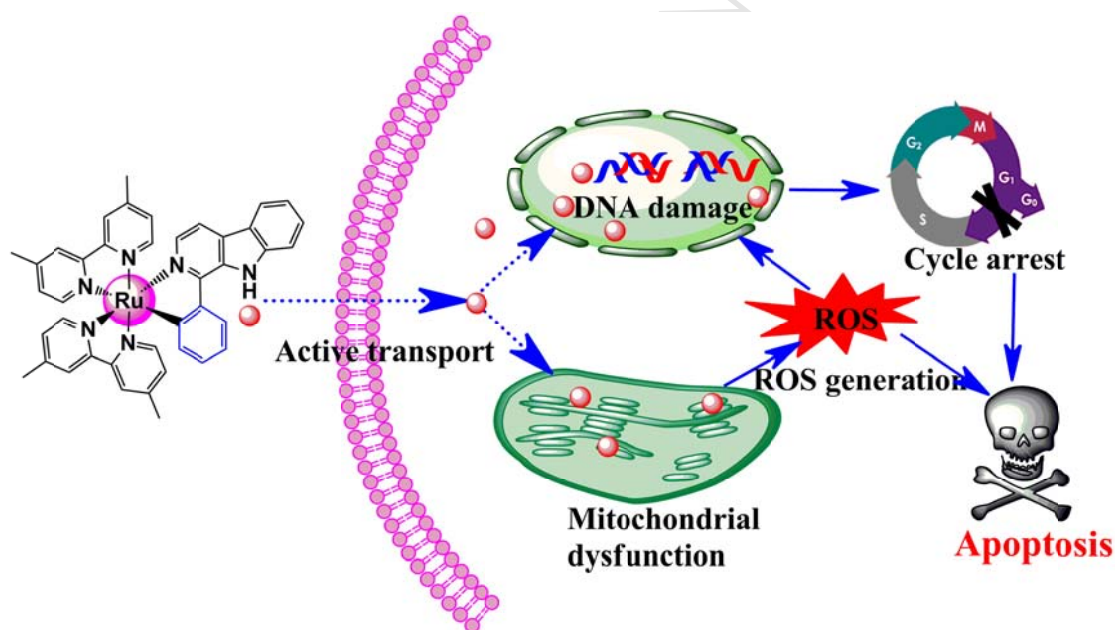
Please cite this article as: J. Chen, F. Peng, Y. Zhang, B. Li, J. She, X. Jie, Z. Zou, M. Chen, L. Chen, Synthesis, characterization, cellular uptake and apoptosis-inducing properties of two highly cytotoxic cyclometalated ruthenium(II) β -carboline complexes, *European Journal of Medicinal Chemistry* (2017), doi: 10.1016/j.ejmech.2017.09.007.

This is a PDF file of an unedited manuscript that has been accepted for publication. As a service to our customers we are providing this early version of the manuscript. The manuscript will undergo copyediting, typesetting, and review of the resulting proof before it is published in its final form. Please note that during the production process errors may be discovered which could affect the content, and all legal disclaimers that apply to the journal pertain.

Graphical Abstract

Synthesis, characterization, cellular uptake and apoptosis-inducing properties of two highly cytotoxic cyclometalated ruthenium(II) β -carboline complexes

The cellular uptake, in vitro cytotoxicities, cell cycle arrest and apoptosis-inducing mechanism of two new cyclometalated ruthenium(II) β -carboline complexes have been extensively explored by ICP-MS, MTT assay, flow cytometry, inverted fluorescence microscope as well as western blotting experimental techniques.



Synthesis, characterization, cellular uptake and apoptosis-inducing properties of two highly cytotoxic cyclometalated ruthenium(II) β -carboline complexes

Jincan Chen^{a,b}, Fa Peng^c, Yao Zhang^c, Baojun Li^c, Ji She^c, Xinming Jie^a, Zhilin Zou^d, Man Chen^d, Lanmei Chen^{c*}

^a Analysis Centre of Guangdong Medical University, Zhanjiang 524023, China

^b Guangdong Key Laboratory for Research and Development of Nature Drugs, Guangdong Medical University, Zhanjiang 524023, China

^c School of Pharmacy, Guangdong Medical University, Zhanjiang 524023, China

^d The First Clinical Medical College, Guangdong Medical University, Zhanjiang 524023, China

*Corresponding author. Tel./fax: Tel: 86-759-2388-568

E-mail addresses: lanmeichen@126.com

Abstract

Two new cyclometalated Ru(II) complexes of the general formula $[\text{Ru}(\text{N-N})_2(1\text{-Ph-}\beta\text{C})](\text{PF}_6)$, where N-N = 4,4'-dimethyl-2,2'-bipyridine (dmb, **Ru1**), 2,2'-bipyridine (bpy, **Ru2**), and 1-Ph- β C (1-phenyl-9H-pyrido[3,4-b]indole) is a β -carboline alkaloids derivatives, have been synthesized and characterized. The in vitro cytotoxicities, cellular uptake and localization, cell cycle arrest and apoptosis-inducing mechanisms of these complexes have been extensively explored by 3-(4,5-dimethylthiazol-2-yl)-2,5-diphenyltetrazolium bromide (MTT) assay, inductively coupled plasma mass spectrometry (ICP-MS), flow cytometry, comet assay, inverted fluorescence microscope as well as western blotting experimental techniques. Notably, **Ru1** and **Ru2** exhibit potent antiproliferative activities against selected human cancer cell lines with IC₅₀ values lower than those of cisplatin and other non-cyclometalated Ru(II) β -carboline complexes. The cellular uptake and localization exhibit that these complexes can accumulate in the cell nuclei. Further antitumor mechanism studies show that **Ru1** and **Ru2** can cause cell cycle arrest in

the G0/G1 phase by regulating cell cycle relative proteins and induce apoptosis through mitochondrial dysfunction, reactive oxygen species (ROS) accumulation and ROS-mediated DNA damage.

Key words: Cyclometalated Ru(II) complexes; β -carboline alkaloids; Cytotoxicity; Apoptosis; Mitochondrial dysfunction

1. Introduction

Cisplatin, which discovered in 1969, is one of the foremost and widely used metal based anticancer drugs for cancer therapy [1,2]. However, significant side effects and drug resistance limited its clinical applications and have also stimulated the development of non-platinum metal-based therapeutics [3]. Ruthenium-based complexes have been regarded as one of the most promising alternatives because of their rich synthetic chemistry, variable oxidation states and potential use as therapeutic anticancer agents with low toxicity to normal cells [4,5].

A number of ruthenium compounds show promising anticancer activity, and some of them exhibit a cytotoxic potency similar to or better than that of cisplatin [6-11]. For example, the piano-stool complexes $[(\eta^6\text{-arene})\text{RuCl}(\text{en})]^+$ (en = 1,2-ethylenediamine), exhibit anticancer activities in vitro comparable to that of cisplatin in a number of cancer cell lines [12,13]. The RAPTA complexes $[(\eta^6\text{-arene})\text{-RuCl}_2(\text{pta})]$ (pta = 1,3,5-triaza-7-phosphatricyclo-[3.3.1.1]-decane), are known to have selective activity on metastatic tumors both in vitro and in vivo similar to that of NAMI-A [14,15]. Recently, it has been noted that the cyclometallated Ru(II) complexes, in which one or more of the nitrogen donors of ruthenium complexes are replaced by a carbon donor atom, exhibit promising cytotoxic properties, and some of which are even more efficient than cisplatin [16-18]. Moreover, it has been found that the cyclometalation of Ru(II) complexes can efficiently enhance the lipophilicity of these complexes and significantly improve their cellular uptake [18-20], which are important factors influencing their cytotoxicities.

Some previous works have showed that Ru(II) polypyridyl complexes with

bioactive alkaloids as ligands offers new opportunities for the design of novel anticancer drugs with enhanced activity [21-23]. The β -carboline alkaloids are a class of synthetic and naturally occurring compounds that possess promising biological activity and pharmacological functions including sedative, antiviral, antimicrobial and anticancer activities [24]. It has been reported that β -carboline alkaloids can exert antitumor activities through multiple mechanisms, such as interfering with DNA synthesis [25], inhibiting DNA topoisomerases I and II [26, 27] etc. Some ruthenium(II)- β -carboline complexes with [Ru(tpy)(N-N)(L)] type reported by Chen et al. show anticancer activity against various cancer cells [28]. Another ruthenium(II) β -carboline complex [Ru(tpy)(Nh)₃]²⁺ (Nh=Norharman) also synthesized by this research group exhibits high and selective cytotoxicity induced p53-mediated apoptosis [29]. A series of ruthenium(II) complexes containing a β -carboline alkaloid as ligand reported by Tan et al. can simultaneously induce autophagy and apoptosis in tumor cells, and among of which, the most active drug, complex [Ru(DIP)₂(1-Py- β C)](PF₆)₂ (DIP= 4,7-diphenyl-1,10-phenanthroline), exhibits higher cytotoxic potency than cisplatin [30].

These findings encouraged us to further optimized these Ru(II) β -carboline complexes by improving their cytotoxicity and their water solubility. We focus on the cycloruthenated Ru(II) complex of 1-phenyl-9*H*-pyrido[3,4-*b*]indole (1-Ph- β C). So in this work, two new cyclometalated Ru(II) complexes [Ru(dmb)₂(1-Ph- β C)]⁺ (**Ru1**) and [Ru(bpy)₂(1-Ph- β C)]⁺ (**Ru2**) contained the bioactive β -carboline derivatives as ligands were designed, synthesized and characterized by ESI-MS, ¹H-NMR and UV-Vis. For elucidating the anticancer functions and molecular mechanisms of **Ru1** and **Ru2**, the cytotoxicity, cellular uptake and localization, apoptosis, cell cycle arrest, mitochondrial membrane potential, reactive oxygen species and DNA damage in HeLa cells have been investigated.

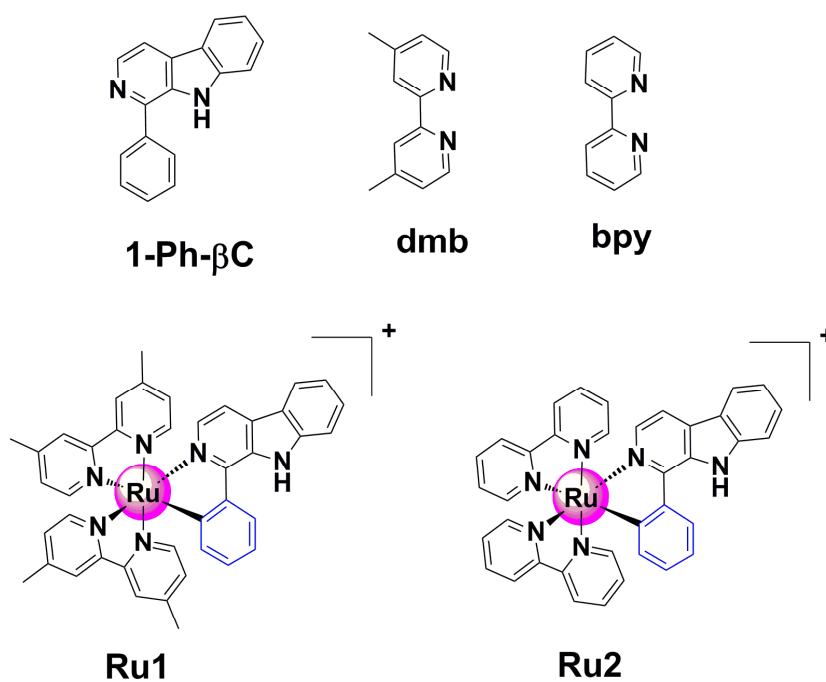


Fig.1. The structures of 1-Ph-βC, dmb, bpy, **Ru1** and **Ru2**.

2. Results and discussion

2.1. Synthesis and characterization

The ligand 1-phenyl-9*H*-pyrido[3,4-*b*]indole (1-Ph-βC) was synthesized according to the literature method [31]. **Ru1** and **Ru2** were prepared by the reaction of $\text{cis-}[\text{Ru}(\text{N-N})_2\text{Cl}_2]$ ($\text{N-N} = \text{dmb, bpy}$) with 1-Ph-βC in ethyl alcohol at room temperature for 12 h. The synthetic route of the ligand 1-Ph-βC and title complexes **Ru1** and **Ru2** was presented in Supporting Information (Fig. S1). The desired Ru(II) complexes were isolated as the chloride salt, and purified by column chromatography. The ligand and the formation of the complexes were confirmed by elemental analysis, ESI-MS and ^1H NMR (Fig. S2-S5). In the ESI-MS spectra for the Ru(II) complexes, all of the expected signals $[\text{M-PF}_6]^+$ were observed. The measured molecular weights were in accordance with expected values.

2.2. UV-visible spectral studies

The stability of **Ru1** and **Ru2** in PBS solutions at 298 K was analyzed by UV-Vis

absorption spectroscopy. As shown in Fig. S6, there is no obvious change in the UV-Vis absorption spectra of Ru(II) complexes during 24 h at 298 K. From Fig. S6 we can see that, both two complexes display several absorption bands in the UV and visible spectral regions. The intense bands occurring between 250 nm and 330 nm are attributed to an intraligand (IL) $\pi-\pi^*$ transition, and the bands at the range of 330–400 nm are attributed to $\pi-\pi^*$ transitions. The bands occurring in the visible region can be assigned to metal-to-ligand charge transfer transitions (MLCT) [32]. In **Ru1**, two intense absorption bands are observed at 449 nm and 509 nm. The latter is attributed to $\text{Ru}^{2+} \rightarrow \text{dmb}$ transitions, and the band centered at 449 nm is assigned to $\text{Ru}^{2+} \rightarrow 1\text{-Ph-}\beta\text{C}$ metal-to-ligand transition [32]. Similar observations are obtained for the **Ru2** complex in the visible region. In **Ru2**, two intense bands are centered at 436 nm and 496 nm.

Electronic absorption spectroscopy is the commonest means to study the interaction of metal complexes with DNA [33]. The spectral profile of the complexes **Ru1** and **Ru2** in the increasing concentration of CT DNA is shown in Fig. S7. As the DNA concentration increased, the metal-to-ligand charge transfer (MLCT) bands of **Ru1** at 449 nm, **Ru2** at 436 nm exhibit hypochromism of about 14.0% and 23.4%, respectively. These spectral characteristics obviously suggest that these complexes interact with DNA most likely through a mode that involves a stacking interaction between the aromatic chromophore and base pairs of DNA. To further evaluate the binding strength of the complexes with DNA, the intrinsic binding constant K_b was determined by monitoring the changes in the absorbance at the MLCT band. The K_b values of **Ru1** and **Ru2** are $4.6 \times 10^3 \text{ M}^{-1}$ and $3.1 \times 10^4 \text{ M}^{-1}$, respectively. These values are smaller than that of $[\text{Ru}(\text{bpy})(\text{phpy})(\text{dppz})]^+(8.5 \times 10^5 \text{ M}^{-1})$ [17], $[\text{Ru}(\text{bpy})_2(1\text{-Py-}\beta\text{C})]^{2+}$ ($1.08 \times 10^6 \text{ M}^{-1}$) [30] and ruthenium methylimidazole complex $[\text{Ru}(\text{MeIm})_4(\text{p-cpip})]^{2+}$ ($5.5 \times 10^5 \text{ M}^{-1}$) [34]. Moreover, it is suggest that complex **Ru1** shows the less binding strength with CT-DNA than complex **Ru2** because of the steric hindrance caused by the methyl groups present at the 4 and 4' positions of the ancillary ligand dmb [35].

2.3. Cytotoxicity assay *in vitro*

Table 1

IC₅₀ values (μM) of **Ru1** and **Ru2** against the selected human cancer cell lines^a.

Complex	IC ₅₀ (μM)					
	A549	HeLa	NCI-H460	HepG-2	MCF-7	BEAS-2B
cis-[Ru(dmb) ₂ Cl ₂]	>200	>161 ± 5.5	>200	>168 ± 6.2	>200	--
cis-[Ru(bpy) ₂ Cl ₂]	>200	>200	>200	>181 ± 7.2	>200	--
1-Ph-βC	79.5 ± 2.6	45.8 ± 3.8	75.2 ± 3.2	102.2 ± 2.8	99.7 ± 3.8	>100
Ru1	2.2 ± 0.2	1.9 ± 0.4	3.8 ± 0.5	10.3 ± 1.2	17.2 ± 2.2	10.6 ± 0.6
Ru2	3.6 ± 0.3	3.4 ± 0.3	4.9 ± 0.8	15.8 ± 2.1	18.4 ± 1.2	11.2 ± 0.5
Ru-Py ^b [30]	--	61.2 ± 3.9	--	86.2 ± 12.3	102.2 ± 14.5	--
Cisplatin	27.2 ± 1.4	18.2 ± 1.2	33.2 ± 2.2	30.1 ± 2.0	16.2 ± 0.9	13.2 ± 0.7

^a Cell viability was determined by MTT assay after treatment for 48 h.

^b Ru-Py = [Ru(bpy)₂(1-Py-βC)](PF₆)₂, 1-Py-βC = 1-(2-pyridyl)-β-carboline.

The ligand 1-Ph-βC, two Ru(II) synthetic precursors cis-[Ru(dmb)₂Cl₂] and cis-[Ru(bpy)₂Cl₂], and corresponding cyclometalated Ru(II) complexes **Ru1** and **Ru2** were evaluated against five selected human cancer cell lines (lung adenocarcinoma cell A549, human lung cancer NCI-H460, hepatocellular carcinoma HepG2, breast cancer MCF-7 and cervical cancer HeLa). For comparison, the toxicity of cisplatin was also evaluated. As a control, the toxicity of these complexes was also tested against the normal human cell line (immortalized human bronchial epithelial cells BEAS-2B). Table 1 shows the IC₅₀ values of the different complexes as determined by an MTT assay after a 48 h incubation. Significant differences are observed that exceeded expectations with **Ru1** and **Ru2** exhibiting much higher activities (IC₅₀ values ranged from 1.9 to 18.4 μM) than cis-[Ru(dmb)₂Cl₂] and cis-[Ru(bpy)₂Cl₂], which are almost inactive against all the cell lines tested (IC₅₀ > 200 μM). The ligand 1-Ph-βC presents moderate activities (IC₅₀ values ranged from 45.8 to 102.2 μM).

Notably, against the human cervical cancer cell line HeLa, **Ru1** and **Ru2** display an IC_{50} values (1.9 μ M and 3.4 μ M, respectively) that are over 32- and 18-fold lower than that of non-cyclometalated Ru(II) β -carboline complex Ru-Py (61.2 μ M) [30]. Moreover, the activities of **Ru1** and **Ru2** are about 9-fold and 5-fold higher than that of cisplatin against HeLa cells under the same conditions.

Therefore, our results clearly show that the coordination of the cyclometalated ligand 1-Ph- β C to polypyridyl-Ru(II) centers is a significant strategy to results in more cytotoxic complexes. Interestingly, **Ru1** is more potent than **Ru2** against all the cancer cell lines screened under identical condition at 48 h treatment, especially HeLa cells. Thus, their cytotoxic effect against HeLa cells was further evaluated. Data obtained are revealed in Fig. S8, **Ru1** and **Ru2** at indicated concentrations resulted in marked reduction of the viability of HeLa cells in a concentration- and time-dependent manner. Moreover, we noticed that the order of DNA binding affinity is $K_b(\mathbf{Ru1}) < K_b(\mathbf{Ru2})$, which is not consistent with their antiproliferative activities. So we deduced that DNA may be not the main target of these ruthenium complexes.

2.4. The cellular uptake and localization of Ru(II) complexes

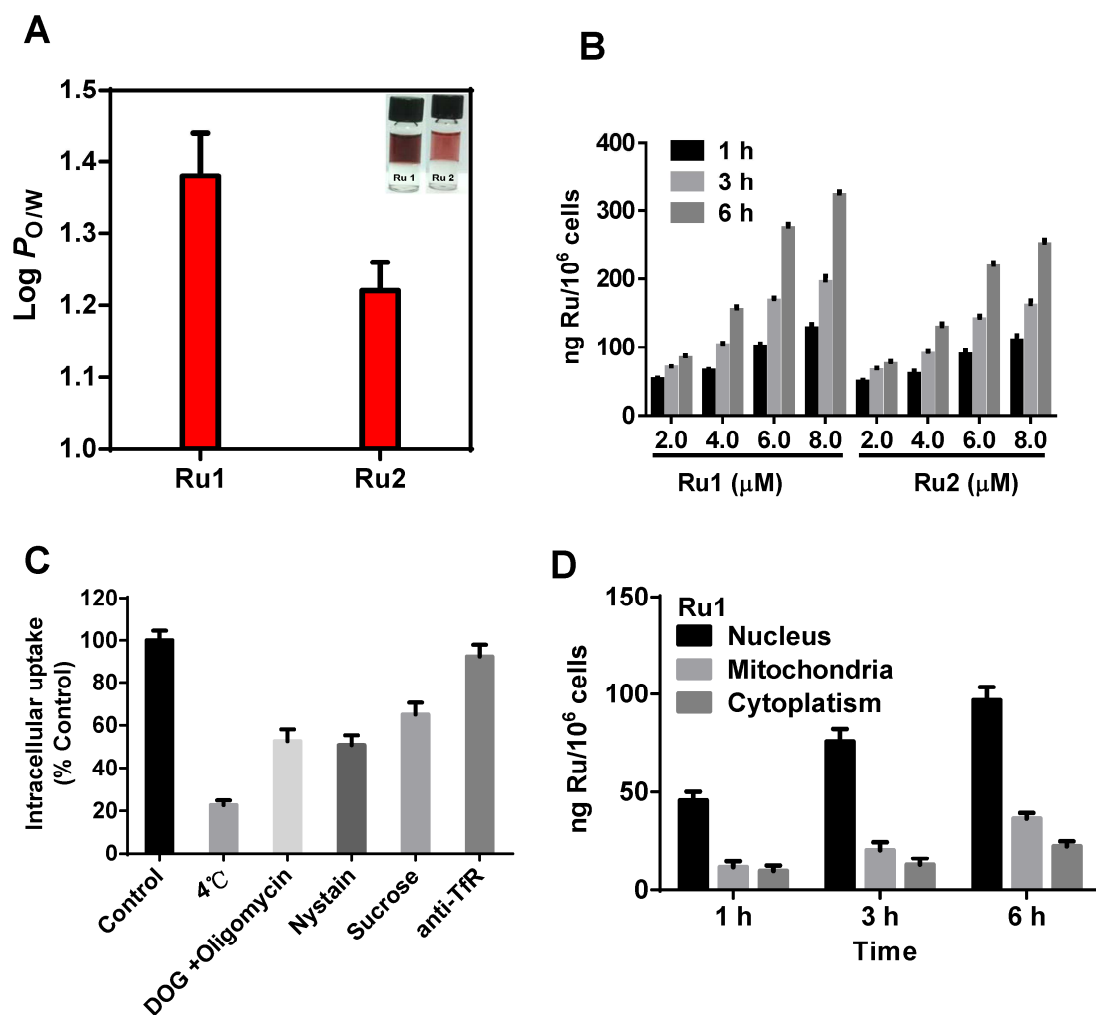


Fig.2. (A) The $\log P_{o/w}$ values of **Ru1** and **Ru2**. (B) Cellular ruthenium concentrations determined in HeLa cells after 1, 3 and 6 h incubated with **Ru1** and **Ru2** at 2, 4, 6, 8 μM , respectively. (C) Intracellular uptake of **Ru1** in HeLa cells under different endocytosis-inhibited conditions. Before 6 h incubation of **Ru1** (4 μM), cells were incubated with specific endocytosis inhibitors, see the experimental section for details. (D) Subcellular distribution of **Ru1** in HeLa cells after incubated with 4 μM of **Ru1** for different times.

It is well known that lipophilicity of an anticancer agent has a vital influence on its cytotoxicity. For some ruthenium [30,36,37] and platinum based compounds [38,39], increasing lipophilicities enhances the cellular uptake and, consequently, the cytotoxic activities. Oil–water partition coefficient ($\log P_{o/w}$) provides a measure of drug lipophilicity, which indicates the ability of the molecule to pass through cell

membranes. “shake-flask” method was used to evaluate the $\log P_{o/w}$ values of **Ru1** and **Ru2** by using ICP-MS. As shown in Fig. 2A, both **Ru1** and **Ru2** exhibit positive $\log P_{o/w}$ values, showing them to be lipophilic in nature. Moreover, **Ru1** ($\log P_{o/w} = 1.38 \pm 0.06$) displays higher $\log P_{o/w}$ value than **Ru2** ($\log P_{o/w} = 1.22 \pm 0.04$). Such result is in accordance with the reported that a positive correlation between hydrophobicity and cytotoxic activity for several classes of metal-based anticancer complexes [30,40-42].

The cellular uptake characteristics of transition metal-based drugs are considered to be one important factor influencing their cytotoxicity [43-45]. To investigate a possible relationship between the dose of cellular uptake and cytotoxic activities of title complexes, the quantitative determination of the ruthenium level inside the HeLa cells has been performed by ICP-MS, and the results were represented as ng of Ru per 10^6 cells. As shown in Fig. 2B, the cellular uptake of **Ru1** and **Ru2** exhibit a significantly dose- and time-dependent manner. In addition, **Ru1** displays higher cellular uptake than that of **Ru2** in all of the test times and drug concentrations, which is positively correlated to their cytotoxicity and lipophilicity.

The approaches of drugs entry into cells have important effect on their bioactivities. To elucidate the anticancer mechanism of title complexes, we investigate the routes of the cellular entry. Normally, small drug molecules enter into cells mainly through two pathways, namely, energy-dependent (such as endocytosis and active transport) and non-energy-dependent (facilitated diffusion) [46,47]. To get more insight into the internalization pathway of **Ru1**, we treated HeLa cells with **Ru1** at low temperature (4 °C) or pretreated with oligomycin in combination with DOG, which can block adenosine 5'-triphosphate (ATP) production to discriminate between passive and active mechanisms. As shown in Fig. 2C, low temperature or oligomycin in combination with DOG can strongly inhibit the cellular uptake of **Ru1**, indicating that the energy-dependent active transport is involved in the cellular uptake of **Ru1**. Endocytosis is the most common energy-dependent method. Next, we further analyzed the internalization pathway of **Ru1** in the presence of two endocytosis inhibitors nystatin (clathrin-mediated endocytosis) and sucrose (lipid raft-mediated

endocytosis) [48]. After treatment with both endocytosis inhibitors, we found that cellular uptake level of **Ru1** was significantly reduced in the nystain group and moderately decreased in the sucrose group. These results suggested **Ru1** can be transported into the cells mainly through clathrin-mediated endocytosis pathway.

It is widely considered that TfR, a transmembrane glycoprotein, is overexpressed on the membrane of many cancer cells. TfR-directed targeting cellular uptake has been regarded as an efficient way for delivery of metal-based agents to malignant tissues [49,50]. Guo et al find that Tf/TfR serves as a mediator enhanced the delivery of organometallic Ru(II) complexes into tumor cells [50]. Thus, we speculate that the intracellular uptake of **Ru1** in HeLa cancer cell lines may associate with its transferrin receptor (TfR) expression profiles. The results in Fig. 2C demonstrate that the intracellular uptake of **Ru1** is barely blocked by pretreatment of anti-TfR, indicating TfR-mediated endocytosis is not involved in the uptake of **Ru1** in HeLa cells.

In addition, the subcellular distribution of **Ru1** in HeLa cells was further determined by ICP-MS. Fig. 2D showed that **Ru1** was predominantly accumulated in the nuclei and only a small fraction of complex was found in mitochondria and cytoplasm, which implied the localization of **Ru1** in the nucleus. At a dose of 4 μ M, treatment with **Ru1** for 6 h, nearly 80% of **Ru1** within the HeLa cells was localized in the nuclei. These results suggest that the cyclometalated complex **Ru1** is a nuclei-targeting Ru(II) complex, like cyclometalated Ru(II) complex, [Ru(bpy)(phpy)(dppz)]⁺ [17].

2.5. Ru(II) complexes induce cell cycle arrest by regulating cell cycle regulatory proteins

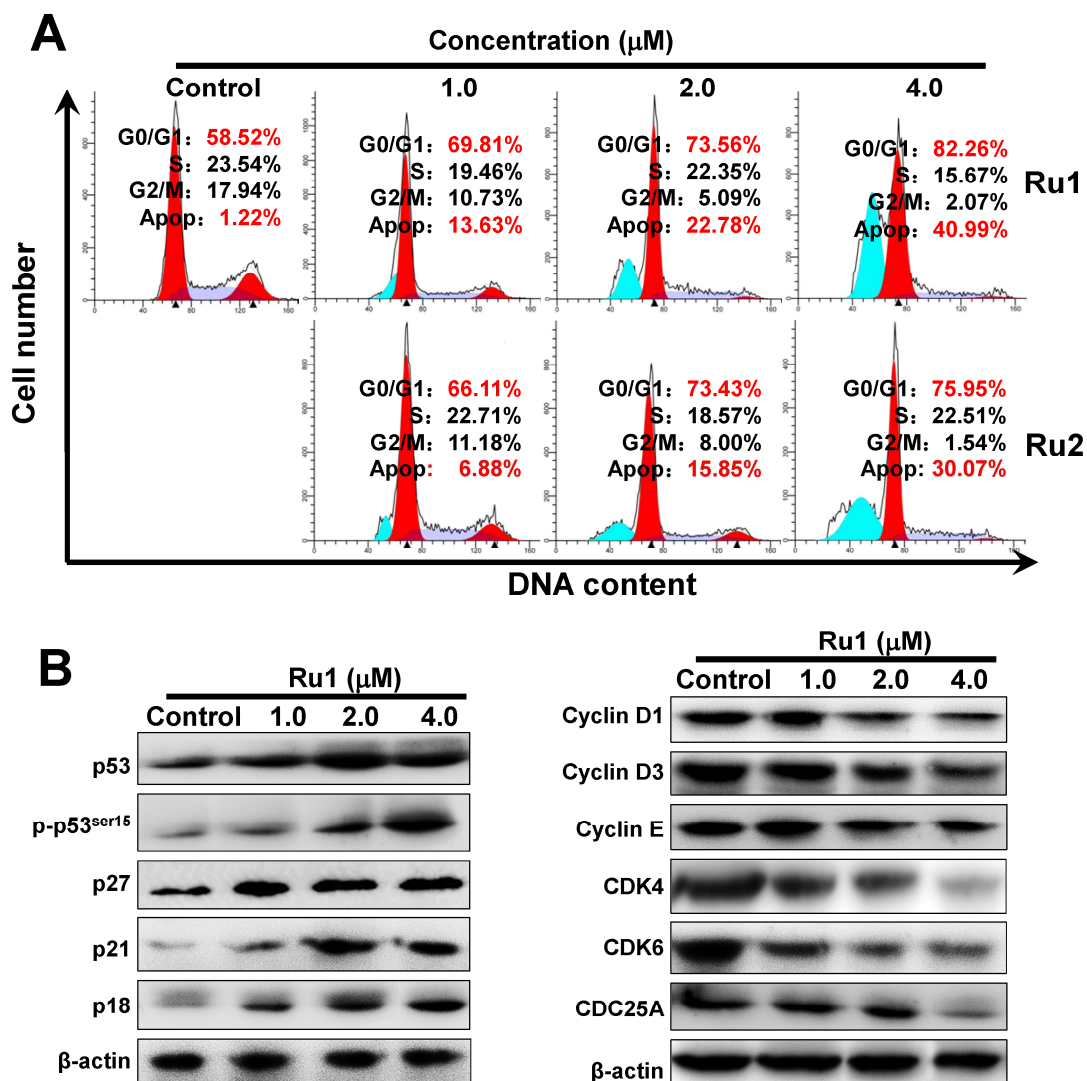


Fig.3. Ru(II) complexes induced cell cycle arrest in HeLa cells. (A) Cell cycle distribution was performed by PI staining after co-incubated with **Ru1** and **Ru2** for 24 h. (B) The effects of **Ru1** on the expression levels of cell cycle relative proteins were performed by western blotting, β -actin was used as internal control. HeLa cells were treated with various concentrations of **Ru1** for 24 h.

It is reported that inhibition of cancer cell proliferation by cytotoxic drugs could be the result of cell cycle arrest, apoptosis or their combination [51]. To investigate whether the anti-proliferative effect of **Ru1** and **Ru2** on HeLa cells was triggered by cell cycle arrest, the cell cycle phase ratio was measured by flow cytometry with propidium iodide (PI) staining. As shown in Fig. 3A, for both **Ru1** and **Ru2** treatment groups, the percentage of cells is increased at G0/G1 phase and decreased at S and

G2/M phases in a concentration-dependent manner. In addition, Fig. 3A also displays that exposure of the HeLa cells to title complexes results in marked dose-dependent increase in the proportion of apoptotic cells as reflected by the subdiploid peak (sub-G1). The value of sub-G1 of **Ru1** treatment group varies from 13.63% (1.0 μ M) to 40.99% (4.0 μ M) with increasing treated concentration. For **Ru2** treatment group, this value varies from 6.88% (1.0 μ M) to 30.07% (4.0 μ M). Meanwhile, Fig. S9 shows that the cells in the sub-G1 phase in these **Ru1**-treated groups also significantly increase in a time-dependent manner, when compared with DMSO treated control. Obviously, these results demonstrate that the antiproliferative effect induced by **Ru1** and **Ru2** on HeLa cells occurs in G0/G1 phase.

To investigate the molecular basis by which Ru(II) complexes inhibited the G0/G1 transition in cancer cells, we treated cells with **Ru1** and then analyzed the expression of proteins involved in cell cycle regulation. We found that **Ru1** treatment inhibited Cyclin D1/D3 and cyclin E expression and reduced the expression of CDK4 and CDK6; in contrast, p27, p21 and p18 were increased in HeLa cells (Fig. 3B). Cyclin D and cyclin E (along with CDK2, CDK4, and CDK6) play important roles in the progression of cells through the G1 phase of the cell cycle [52]. The Cip/Kip family proteins p27, p21 and p18 are well-known CDK inhibitors, up-regulation the expression levels of those can block G1-S transition [53]. The expression level of cell division cycle 25A (CDC25A), which acts as an upstream regulator of the CDK/cyclin complex [54], was significantly inhibited by **Ru1**. **Ru1** treatment also increased the expression of p53 and phosphorylated p53 at ser15 site (p-p53ser15), which is tumor suppressor proteins, up-regulation the expression levels of those can promote the cell cycle arrest and induce cell apoptosis [55,56].

2.6. Ru(II) complexes induce HeLa cell apoptosis

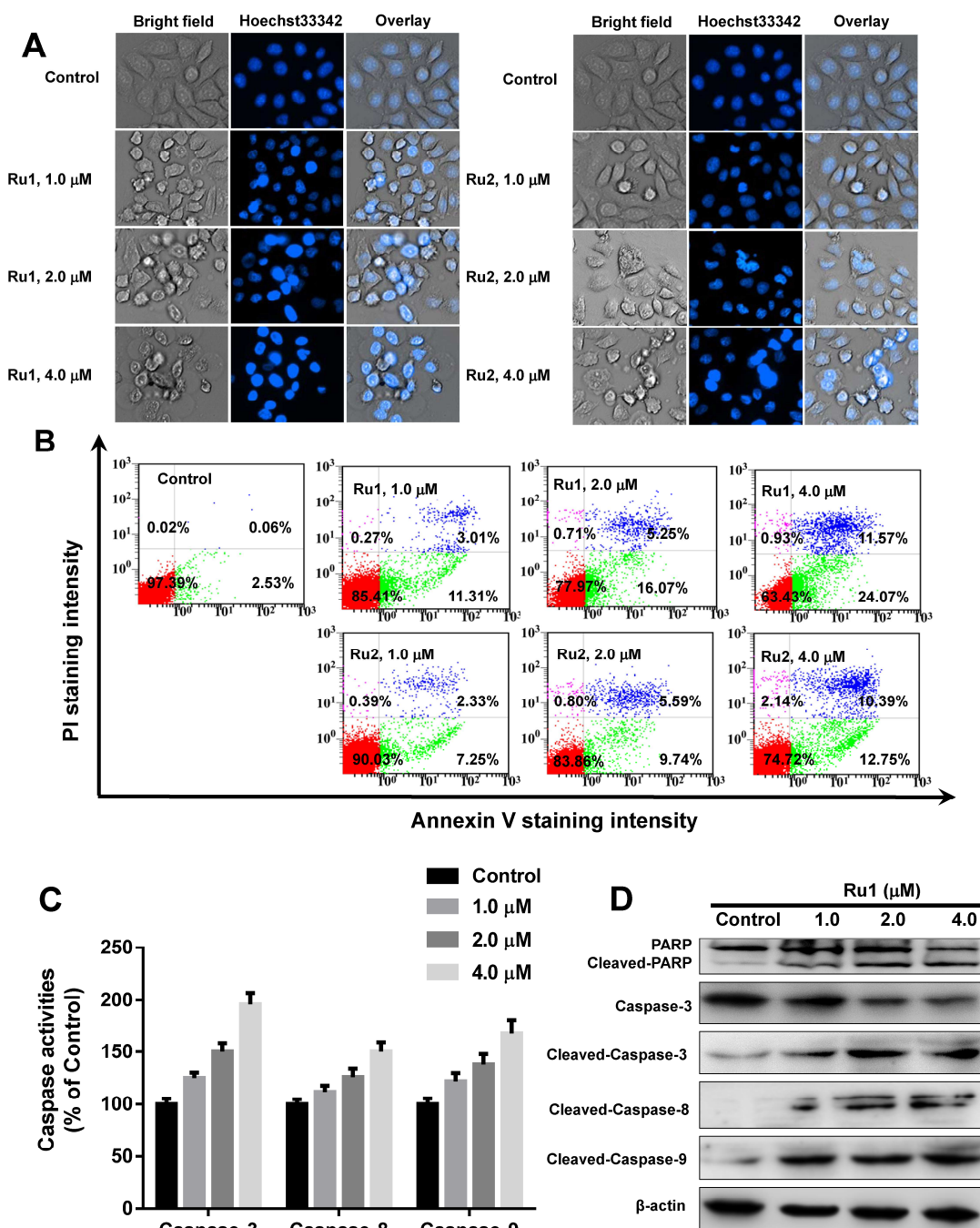


Fig.4. Ru(II) complexes induce HeLa cells apoptosis. (A) HeLa cells stained with Hoechst 33342 after treatment of Ru(II) complexes at indicated concentrations for 24 h. (B) HeLa cells apoptosis was detected by annexin V/PI assay after co-incubation with various concentrations of Ru(II) complexes for 24 h. (C) Caspase activities were measured by using specific fluorescent substrates for caspase-3/8/9. (D) The expression levels of caspase-3, PARP and cleaved caspase-3/8/9 and PARP were evaluated in a dose-dependent manner with Ru1 treatment for 24 h. β -actin was used as internal control.

Cell cycle arrest triggered by various stimulating factors may result in the blockage of cell division and apoptosis. To determine whether or not **Ru1** and **Ru2** could induce chromatin condensation and fragmentation, both of which were recognized as morphological features of apoptosis, the Hoechst 33342 staining technique for fluorescence microscopy was performed. HeLa cells were treated with different concentrations of Ru(II) complexes for 24 h, and then photographed using an inverted fluorescence microscope. As shown in Fig. 4A, the cells with apoptotic features such as nuclear fragmentation, chromatin condensation and plasma membrane blebbing are observed. In addition, the apoptosis assay was also performed by acridine orange/ethidium bromide (AO/EB) dual-staining method. AO is a vital dye and can stain both live and dead cells and shows green fluorescence. EB stains only apoptotic or necrotic cells that have lost their membrane integrity and appear red fluorescence. Fig. S10 displays that, in control cells, the normal morphology and homogeneous green fluorescence are obtained. When cells are pre-incubated with **Ru1** and **Ru2**, the orange or red fluorescence, that are the clearly morphological features of apoptosis, are observed. These preliminary results indicate that both **Ru1** and **Ru2** can induce apoptosis of HeLa cells.

To further confirm the nature of cell death induced by **Ru1** and **Ru2**, annexin V-FITC/PI staining was performed, and the results were analyzed by using flow cytometry. Fig. 4B shows that pre-incubation of HeLa cells with different concentrations of **Ru1** or **Ru2** for 24 h enhances the percentage of apoptotic cells. Comparing the apoptotic effect, we can find that **Ru1** displays more effective apoptotic activity than **Ru2** under identical conditions, which is consistent with their cytotoxic activity.

A large number of evidence has indicated that caspases play vital roles for initiation and performance of apoptosis [57-59]. Apoptotic pathways can be divided into the extrinsic and intrinsic pathways, which are dependent on the cleavage of caspases [60]. Caspase-3 is a vital regulatory protein of cell apoptosis, the activation of which lead to the cleavage of poly ADP-ribose polymerase (PARP), thus to induce the cells

apoptosis [61]. To further clarify the mechanism of cells apoptosis induced by **Ru1**, the activities of caspase-3, -8 and -9 were examined by using specific fluorescent substrates. As shown in Fig. 4C, pre-incubation of HeLa cells with different concentration of **Ru1** exhibits dramatic enhancement in caspase-3, -8 and -9 activities. Besides, the results of western blot assay in Fig. 4D illustrate that the expression levels of cleaved-PARP, cleaved caspase-3, cleaved caspase-8 and cleaved caspase-9 increase in a dose- dependent manner, and the expression level of total caspase-3 decrease in a dose- dependent manner, which suggesting both extrinsic and intrinsic apoptosis pathways are involved in **Ru1**-induced apoptosis in HeLa cells.

2.7. Ru(II) complexes induce mitochondrial dysfunction

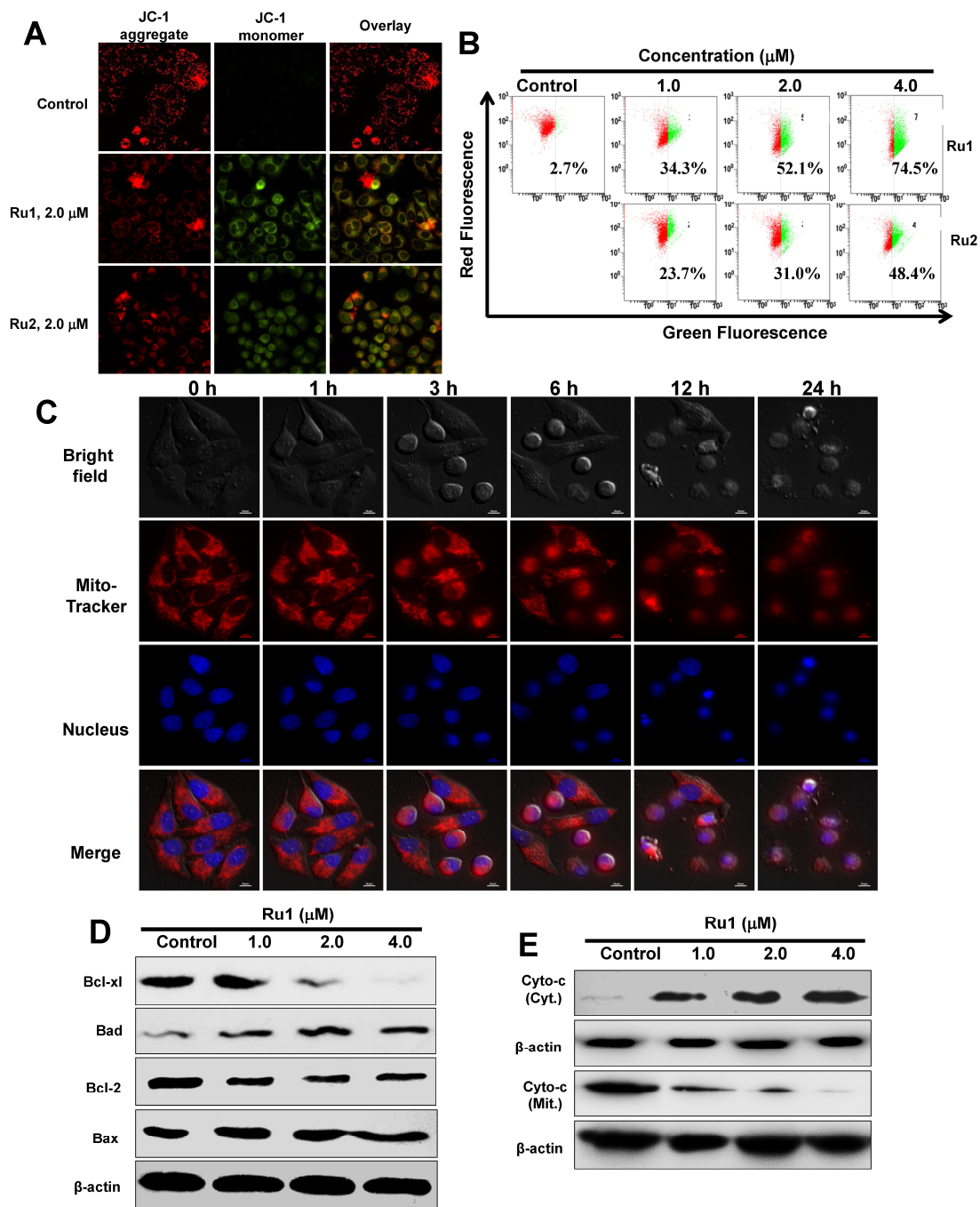


Fig.5. Ru1 and Ru2 induce mitochondrial dysfunction. (A) Fluorescence microscope analysis of cellular MMP level by JC-1 staining after 2 μ M of **Ru1** or **Ru2** treatment for 24 h. (B) Flow cytometry analysis of cellular MMP level after 1, 2 and 4 μ M of **Ru1** or **Ru2** treatment for 24 h. (C) Real-time imaging the same cells treated with 2 μ M of **Ru1** for different times. Cell morphology was captured by differential reflection (DIC) microscope. Mitochondria and nuclei were visualized by red and blue fluorescence, respectively. The bottom panel is DIC images. (D) The expression levels of Bcl-2 family protein were performed in a dose-dependent

manner. β -actin was used as internal control. (E) The expression levels of cytochrome *c* in cytosol and in mitochondria, respectively, were performed after 1, 2, 4 μ M of **Ru1** treatment for 24 h.

Mitochondrion, which plays an important role in apoptosis, can release pro-apoptotic factors such as cytochrome *c* and other apoptosis inducing factors. [17,62]. Mitochondrial dysfunction is involved in apoptotic cell. Generally, the mitochondrial dysfunction is determined by measuring changes in the loss of mitochondrial membrane potential (MMP) using an inverted fluorescence microscope and flow cytometry after staining live cells with 5,5',6,6'-tetrachloro-1,1',3,3'-tetraethylbenzimidazolylcarbo cyanine iodide (JC-1) as fluorescent probe. As shown in Fig. 5A, compared with control, **Ru1** (2.0 μ M) or **Ru2** (2.0 μ M) treatment cause a red to green color shift in most of the treated cells, indicating loss of MMP. The changes of MMP were also detected quantitatively by determining the percentage of the red and green fluorescent intensity using flow cytometry (Fig. 5B). As shown in Fig. 5B, after 6 h of incubation with Ru(II) complexes, the green fluorescence of the JC-1 monomers increase from 2.7% to 74.5% and 48.4% for **Ru1** (4 μ M) and **Ru2** (4 μ M), respectively.

To determine whether or not, mitochondria are pivotal in controlling cell growth and death, real-time living cell experiment was carried out. We observed the changes of mitochondria (stained by Mito-Tracker; nuclei stained by DAPI) in HeLa cells treated with 2.0 μ M of **Ru1** for different time intervals. As shown in Fig. 5C, obvious mitochondrial fragmentation, nuclear condensation and cytoplasmic shrinkage can be observed after treatment for 3 h, further indicating the mitochondrial dysfunction.

Additionally, western blot analysis was performed to confirm the mitochondrial pathways in apoptosis which induced by **Ru1**. The results in Fig. 5D indicate that treatment with **Ru1** dose dependently suppresses the expression of the anti-apoptotic protein Bcl-xl and Bcl-2. As a result of these changes, the ratios of Bcl-2/Bax and Bcl-xl/Bad decrease, and thus leading to the release of cytochrome *c* (an apoptosis inducing factor) into the cytosol. Actually, the experimental results suggest that cytochrome *c* of cytosol increase in a dose-dependent manner, while those in

mitochondria decrease (Fig. 5E). This result further confirms that **Ru1** induces mitochondrial dysfunction and the mitochondrial pathway is involved in **Ru1**-induced apoptosis in HeLa cells.

2.8. Ru(II) complexes induce intracellular ROS accumulation

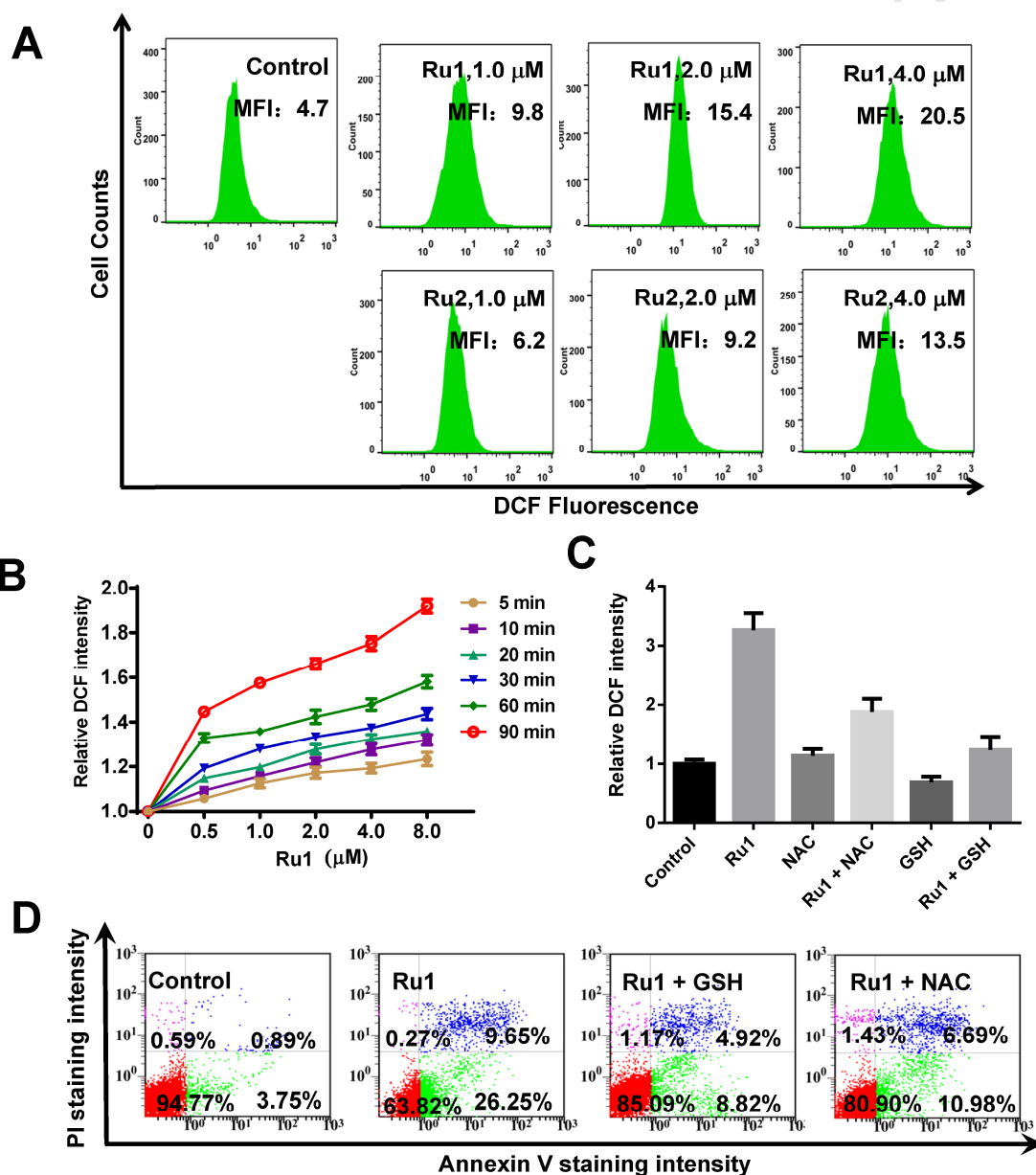


Fig.6. (A) ROS generation was determined by flow cytometry, HeLa cells stained with DCFH-DA after Ru(II) complexes treatment for 6 h. (B) The cellular ROS level was detected by microplate reader after exposure to **Ru1** for different times in HeLa cells. (C) Flow cytometry analysis of

cellular ROS level by DCFH-DA staining after 2.0 μM of **Ru1** treatment for 6 h. (D) Cells apoptosis were detected by flow cytometry, HeLa cells were treated with **Ru1** for 24 h with or without pretreatment of NAC and GSH.

ROS, which regard as mediators of apoptosis, are important for the induction of apoptosis in many cancer cells [63,64], and could enter the nucleus to cause DNA damage [65]. To investigate whether Ru(II) complexes treatment could increase the ROS level in HeLa cells, the cellular ROS level was detected by using an inverted fluorescence microscope and flow cytometry after cells stained with a DCFH-DA fluorescent dye. Fig. S11A displays that, compared with DMSO-treated control, HeLa cells exhibit obvious green fluorescence when treated with 2.0 μM of **Ru1** or **Ru2** for 6 h, which indicates an increase in the cellular ROS level. A similar result is also obtained by flow cytometry. As shown in Fig. 6A, at a dose of 4 μM , treatment with **Ru1** or **Ru2** for 6 h results in marked increase of the mean fluorescent intensity (MFI) by approximate 4.3- and 2.8- fold than control group, respectively.

Data obtain from Fig. 6B suggest that **Ru1** significantly enhances cellular ROS level in a dose- and time-dependent manner, and the ROS is detected as early as 5 min, indicating ROS as an early event in respond to **Ru1**-induced apoptosis. To inquire into the contribution of ROS in **Ru1**-induced HeLa cells apoptosis, two antioxidants N-acetyl-L-cysteine (NAC) and glutathione (GSH) were used. As shown in Fig. 6C, both NAC and GSH can substantially suppress the intracellular ROS levels. The percentage of apoptotic cells was detected by Annexin V staining assay after **Ru1** treatment with or without antioxidants NAC or GSH. From Fig. 6D, we can see that the percentage of apoptosis cells induced by **Ru1** obviously reduces when ROS is inhibited by antioxidants. Meanwhile, Fig. S11B presents that both NAC and GSH obviously increase cell viability. Taken together, these results suggest that activation of ROS-generating by Ru(II) complexes plays an important role in inducing apoptotic in HeLa cells.

2.9. Ru(II) complexes trigger DNA damage

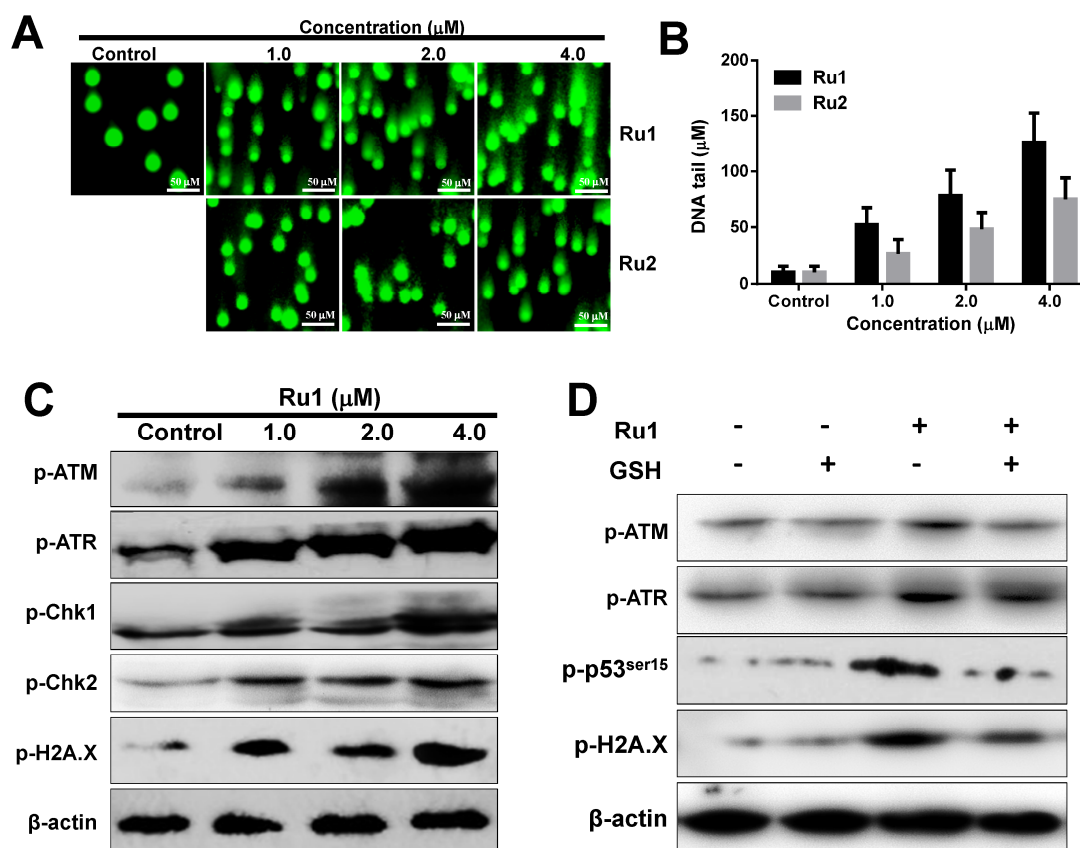
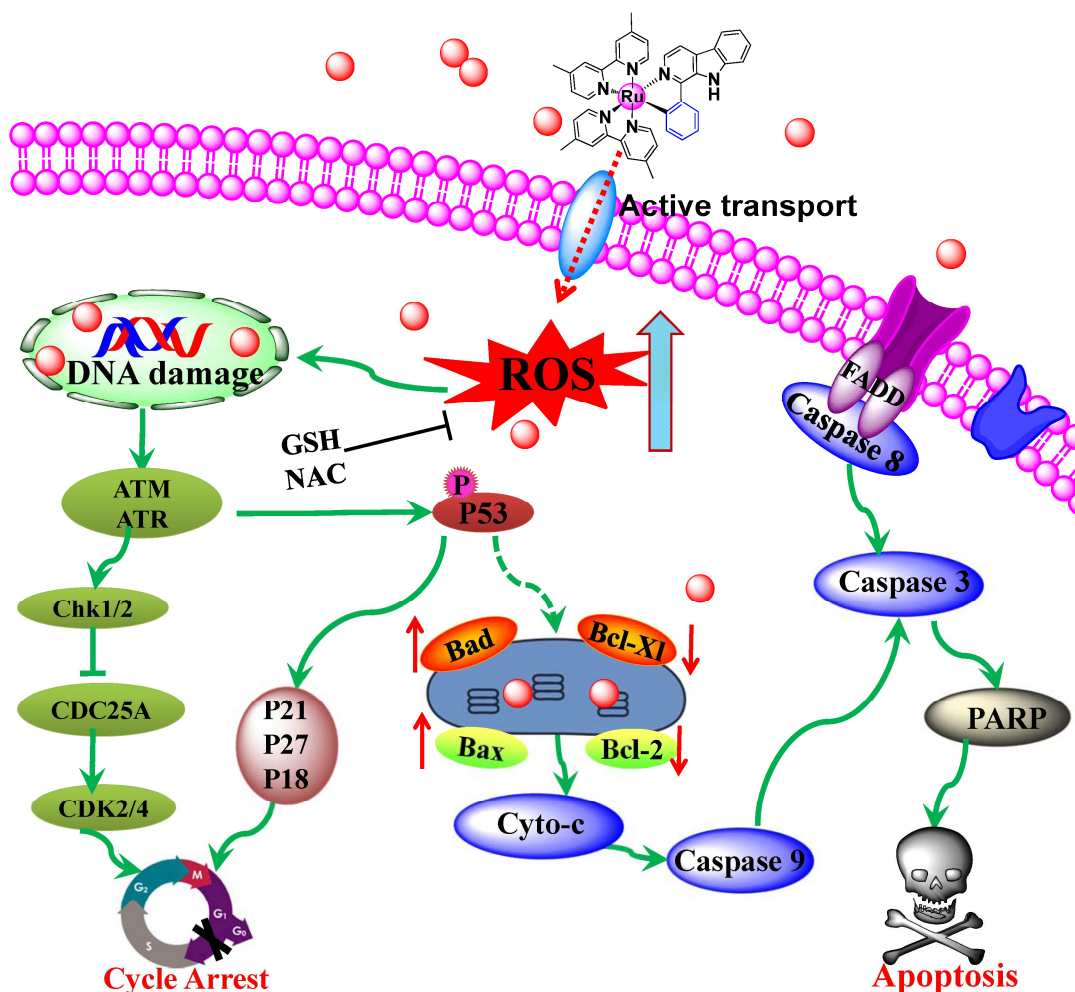


Fig.7. DNA damage was examined by comet assay and western blotting experiment. (A) HeLa cells were treated with various concentration of **Ru1** or **Ru2** for 24 h, DNA fragmentation was examined by comet assay. (B) Quantification of DNA tails in the comet assay. The length of DNA tails in microscopy images was quantified by ImageJ. (C) The expression levels of phosphorylated proteins ATM, ATR, Chk1, Chk2, H2A.X were performed by western blotting. (D) Western blotting analysis of expression levels of DNA damage proteins in HeLa cells in the presence of GSH, β -actin was used as internal control.

A number of Ru(II) complexes can trigger DNA damage, also some Ru(II) compounds exhibit photo-induced DNA cleavage activity [34,66,67]. DNA damage is regarded as a hallmark of apoptosis [68,69]. It has been reported that excess intracellular ROS can attack DNA, resulting in DNA damage and activation of various damage sensor proteins such as ATM, Histone proteins, and the tumor

suppressor gene p53 [70]. In this work, to study whether or not **Ru1** can induce DNA damage and activate DNA damage sensor proteins, such as Histone protein, which is a marker of DNA double-strand breaks, single cell gel electrophoresis (comet assay) and western blotting assay were performed. Comet assay is a simple and rapid method for assessing DNA damage generated by DNA-targeting agents in single cells, and the length of the comet tail represents the level of DNA damage. As shown in Fig. 7A, in the control, HeLa cells fail to show a comet like appearance. After incubation with **Ru1** (1.0 μM) and **Ru2** (1.0 μM) for 24 h, HeLa cells exhibit well-formed comet tails, indicating that severe DNA damage has occurred. With extension of the concentration to 4.0 μM , statistically significant comet tails appear, suggesting that more DNA damage has occurred. The quantification of comet tails in the comet assay is shown in Fig. 7B. The length of comet tails in microscopy images was quantified by ImageJ. Differences. Fig. 7B suggests that **Ru1** induces more DNA damage than that of **Ru2** induces.

In addition, **Ru1**-induced DNA damage was further confirmed by western blotting assay (Fig. 7C), as evidenced by the up-regulation of the phosphorylation levels of H2A.X (Ser¹³⁹), ATM (Ser¹⁹⁸¹) and ATR (Ser⁴²⁸), which are the DNA damage markers. Meanwhile, Chk1 and Chk2 are activated, as evidenced by the increase of the phosphorylation levels of Chk1 and Chk2. Interestingly, when an antioxidant GSH is added to the cells which incubated with **Ru1**, the levels of p-H2A.X (Ser¹³⁹), p-p53 (Ser¹⁵), p-ATM (Ser¹⁹⁸¹) and p-ATR(Ser⁴²⁸) are down-regulate (Fig. 7D). These results demonstrate that **Ru1** induces DNA damage through ROS overproduction, like ruthenium (II) imidazole complex $[\text{Ru}(\text{MeIm})_4(\text{p-cpip})]^{2+}$ [34].



Scheme 1: Proposed apoptosis pathways induced by **Ru1** in HeLa cells.

3. Conclusions

In this work, we synthesized two new cyclometalated Ru(II) complexes $[\text{Ru}(\text{dmb})_2(1\text{-Ph-}\beta\text{C})]^+$ (**Ru1**) and $[\text{Ru}(\text{bpy})_2(1\text{-Ph-}\beta\text{C})]^+$ (**Ru2**). Both **Ru1** and **Ru2** display IC_{50} values much lower than those of cisplatin and other non-cyclometalated Ru(II)- β -carboline complexes $[\text{Ru}(\text{N-N})_2(1\text{-Py-}\beta\text{C})](\text{PF}_6)_2$ (N-N = bpy, phen). Notably, the antiproliferative activities of **Ru1** and **Ru2** are much higher than those of precursors cis- $[\text{Ru}(\text{bpy})_2\text{Cl}_2]$, cis- $[\text{Ru}(\text{dmb})_2\text{Cl}_2]$ and 1-Ph- βC , suggesting that the significantly higher anticancer activity has been achieved by complexation of Ru(II) polypyridyl moieties with 1-Ph- βC . The hydrophobicity, cellular uptake efficiency and cytotoxic effect on tumor cells of **Ru1** and **Ru2** are significantly correlated. The

higher lipophilic of **Ru1**, shows higher cellular uptake efficiency and is more activity than **Ru2**.

The cellular uptake and localization exhibit that Ru(II) complexes can be transported into the cells mainly through clathrin-mediated endocytosis pathway, and these complexes can accumulate in the cell nuclei. Hoechst 33342 staining and AO/EB dual-staining demonstrate that both **Ru1** and **Ru2** can effectively induce apoptosis of HeLa cells. In addition, these complexes enhance the level of intracellular ROS and induce a decrease of MMP. And further studies show that ROS play vital roles in **Ru1**-induced apoptosis and cell viability. Western blotting analysis show that **Ru1** activates Caspase-3/8/9, increases the level of the pro-apoptotic proteins Bad and Bax, decreases the levels of the anti-apoptotic protein Bcl-x1 and Bcl-2, thus leads to the release of cytochrome *c* in HeLa cells. Moreover, comet assay and western blotting analysis indicate that **Ru1** can induce DNA damage as evidenced by the up-regulation of the phosphorylation levels of H2A.X, ATR and ATM, and the latter two further phosphorylates the downstream effectors ChK1/2. Next, the phosphorylated effectors downregulate the expression of CDC25A, thereby inhibiting the CDK2/4 kinases and subsequently leading to cell cycle arrest at the G0/G1 phase.

Taking all these results together, we conclude that **Ru1** and **Ru2** can induce cell apoptosis in HeLa cells mainly through mitochondrial dysfunction, intracellular ROS accumulation and ROS-mediated DNA damage. The schematic diagram of this proposed apoptosis pathway induced by **Ru1** in HeLa cells is illustrated in Scheme 1. These results will be helpful for design and synthesis of new cyclometalated Ru(II) complexes as potent anticancer drugs.

4. Experimental section

4.1 Materials and general methods

All reagents and solvents were purchased commercially and used without further purification unless specifically noted, and all aqueous solutions were prepared with doubly distilled water. 1-phenyl-9*H*-pyrido[3,4-*b*]indole (1-Ph- β C) [31] and

cis-[Ru(L)₂Cl₂].2H₂O (L = dmb, bpy) were prepared according to the literature methods [71]. Annexin V-FITC Apoptosis Detection Kit, QuantiPro™ BCA Assay Kit, ECL™ Start Western Blotting Detection Reagent, DMSO, MTT, phosphate buffered saline solution (PBS), DNA (CT-DNA), PI, JC-1, GSH, NAC, DCFH-DA were purchased from Sigma-Aldrich (St. Louis, MO, USA). Cisplatin was purchased from Acros. Cell Mitochondria Isolation Kit and specific caspase substrates were purchased from Beyotime (Shanghai, China). Ruthenium standard solution was purchased from Aladdin Chemistry Co. (Shanghai, China). Primary and secondary antibodies were purchased from Cell Signaling Technology Company. Anti-Transferrin Receptor antibody (anti-TfR antibody) was purchased from Abcam (Shanghai, China). Comet assay reagent kit was purchased from Trevigen (Gaithersburg, MD, USA). Protein bands were visualized using ChemiDoc™ XRS+ Imaging System (Bio-Rad, USA). Flow cytometry was performed by EPICS XL-MCL (BECKMAN COULTER, USA) and microscopic observation was performed by Ti-E (Nikon, Japan). Microanalyses (C, H, and N) were carried out with a Perkin-Elmer 240Q elemental analyser. Electrospray ionization mass spectrometry (ESI-MS) was recorded on an Agilent LC-MS6430B Spectrometer using CH₃CN as mobile phase. ¹H NMR spectra was recorded on a Bruker AVANCE 400 spectrometer (400 MHz) with (CD₃)₂SO as solvent for the complexes at room temperature. All chemical shifts relative to tetramethylsilane (TMS) were given.

4.2. Synthesis and characteristics

4.2.1. Synthesis of [Ru(dmb)₂(1-Ph-βC)] (PF₆) (Ru1)

A mixture of cis-[Ru(dmb)₂Cl₂].2H₂O (0.27 g, 0.5 mmol), 1-Ph-βC (0.12 g, 0.5 mmol), AgNO₃ (0.17 g, 1.0 mmol) and tetramethylammonium hydroxide (0.092 g, 0.5 mmol) were dissolved in anhydrous ethanol (15 mL), and then the mixture was heated at reflux under nitrogen at 25 °C for 24 h to give a clear red solution. Upon completion of the reaction, the red precipitate was obtained by a dropwise addition of saturated aqueous KPF₆ solution. Finally, the red precipitate was dried under vacuum and purified by chromatography over alumina (200 mesh), using

acetonitrile/toluene-(1:2, v/v) as an eluent. Yield: 81.8 %. Anal. calc. for $C_{41}H_{35}F_6N_6PRu$: C 57.41%, H 4.11%, N 9.80%; found: C 57.21%, H 4.09%, N 9.81%. ESI-MS (MeCN): $m/z = 713.2$ ($[M-PF_6]^+$). 1H NMR (400 MHz, DMSO- d_6) δ 11.77 (s, 1H), 8.64 (d, $J = 1.7$ Hz, 1H), 8.56 – 8.37 (m, 4H), 8.14 (d, $J = 7.9$ Hz, 1H), 7.84 – 7.72 (m, 3H), 7.69 – 7.53 (m, 2H), 7.50 (d, $J = 5.8$ Hz, 1H), 7.44 – 7.33 (m, 3H), 7.33 – 7.17 (m, 2H), 7.16 – 7.06 (m, 2H), 6.99 (td, $J = 7.5, 1.4$ Hz, 1H), 6.82 (td, $J = 7.3, 1.1$ Hz, 1H), 6.51 (dd, $J = 7.4, 1.3$ Hz, 1H), 2.51 (s, 3H), 2.44 (s, 3H), 2.37 (s, 6H).

4.2.2. Synthesis of $[Ru(bpy)_2(1-Ph-\beta C)](PF_6)$ (Ru2)

Ru2 was synthesized by a similar procedure to **Ru1**. Cis- $[Ru(bpy)_2Cl_2] \cdot 2H_2O$ was used instead of cis- $[Ru(dmb)_2Cl_2] \cdot 2H_2O$. Yield: 82.1%. Anal. calc. for $C_{37}H_{27}F_6N_6PRu$: C 55.43%, H 3.39%, N 10.48%; found: C 55.37%, H 3.37%, N 10.53%. ESI-MS (MeCN): $m/z = 657.2$ ($[M-PF_6]^+$). 1H NMR (400 MHz, DMSO- d_6) δ 11.82 (s, 1H), 8.81 (dt, $J = 8.4, 1.1$ Hz, 1H), 8.70 (dt, $J = 8.2, 1.1$ Hz, 1H), 8.64 (ddt, $J = 10.5, 8.2, 1.1$ Hz, 2H), 8.47–8.40 (m, 1H), 8.19–8.09 (m, 2H), 8.01–7.96 (m, 1H), 7.96–7.76 (m, 6H), 7.70–7.67 (m, 1H), 7.63–7.55 (m, 3H), 7.41–7.27 (m, 5H), 7.03 (td, $J = 8.0, 7.6, 1.4$ Hz, 1H), 6.85 (td, $J = 7.3, 1.1$ Hz, 1H), 6.47 (dd, $J = 7.4, 1.3$ Hz, 1H).

4.3. Cytotoxicity assay in vitro

Five different tumor cell lines (lung adenocarcinoma cell A549, human lung cancer NCI-H460, cervical cancer HeLa, breast cancer MCF-7, hepatocellular carcinoma HepG2, and cervical cancer HeLa) and one normal cell lines (immortalized human bronchial epithelial cells BEAS-2B) were purchased from American Type Culture Collection (ATCC, Manassas, VA). All cell lines were cultured in Roswell Park Memorial Institute 1640 (RPMI 1640) culture media supplemented with 10 % fetal bovine serum (FBS) and incubated in incubator with 5 % CO_2 at 37 °C unless otherwise noted. The IC_{50} values were determined by MTT assay.

4.4. Lipophilicity measurements

Lipophilicity was determined by liquid–liquid extraction between n-octanol (oil) and NaCl (0.9% w/v) using the flask-shaking method as previously described [34]. Briefly, the ruthenium complex in NaCl (0.9% w/v) was added to an equal volume of n-octanol (oil), and the mixture was shaken for 48 h at 200 rpm at 25 °C to allow partitioning. After centrifuging the sample at 3000 rpm for 10 min, the aqueous layer was used for ruthenium analysis, and the Ru content in the aqueous layer was then measured by ICP-MS and used to calculate the $\log P_{o/w}$ values according to the equation $\log P_{o/w} = \text{Log} ([\text{Ru}]_o / [\text{Ru}]_w)$.

4.5. Cellular uptake

HeLa cells at a density of 5.0×10^5 cells were seeded in 60 mm tissue culture dishes and allowed to reach 70% confluence, then the cells were incubated with the different concentration of Ru(II) complexes for different times. After treatment, the cells were treated with trypsin and collected in centrifugal tubes, and then washed three times with cold PBS. The pellets were completely digested in 3 mL mixture (2 mL, 60% HNO₃ and 1 mL, H₂O₂) for 24 h, and then diluted to 4 mL with ultrapure water. Finally, the amount of Ru taken up by HeLa cells was determined by ICP-MS (NEXION-300X, PerkinElmer, USA) with a 100 ng/mL ruthenium standard solution for drawing a standard line. Ruthenium standard solutions were freshly prepared before each experiment. The water used for ICP-MS analysis was doubly deionized. The uptake of Ru was calculated from the standard curve and expressed as the amount of Ru (ng) taken up per 10^6 cells.

4.6. The mechanism of cellular uptake

HeLa cells were seeded into 60 mm tissue culture dishes for 24 h, and then the cells were pretreated with endocytosis inhibitors oligomycin 5 μM , 2-deoxy-D-glucose (DOG) 50 μM , sucrose 0.25 mM, nystatin 10 $\mu\text{g/mL}$ and anti-TfR (1 $\mu\text{g/mL}$) for 2 h or at 4 °C for 4 h, respectively, before treatment of 4 μM of **Ru1** for 6 h. The control sample was just exposed to 4 μM of **Ru1** at 37 °C for 6 h. Then the

cells were trypsinized and collected. Finally, the intracellular uptake of **Ru1** were determined using ICP-MS.

4.7. Subcellular distribution of Ru(II) complexes

The subcellular distribution of **Ru1** was detected using Cell Mitochondria Isolation Kit according to manufacturer's recommendations. Briefly, after incubation with 4.0 μM of **Ru1** for different times, cells were harvested and washed twice with cold-PBS and re-suspended in the mitochondria isolation buffer for 15 min under low temperature conditions. The suspension was homogenized using a Dounce homogenizer, and then the homogenate was centrifuged at $600\times g$ for 10 min at 4 °C. The pellets (nuclear fraction) were completely digested in 4 mL mixture (3 mL, 95% HNO_3 and 1 mL, H_2O_2), and the supernatant was centrifuged at $11\ 000\times g$ for 10 min at 4 °C. The resulting supernatants (cytoplasmic fractions) and pellets (mitochondrial fractions) were also digested in 4 mL mixture, respectively. Finally, ruthenium element was determined by ICP-MS with a 100 ng/mL ruthenium standard solution for drawing a standard line.

4.8. Cell cycle arrest analysis

Cell cycle distribution and apoptosis were analyzed by flow cytometry analysis as described previously [67,72]. HeLa cells were plated in 6-well plate and incubated for 24 h. Different concentrations of Ru(II) complexes were then added into the wells and incubated for 24 h. After incubation, cells were collected and fixed in 1.5 mL aqueous ethanol (75%, v/v) at -20 °C overnight, and then stained with PI (50 $\mu\text{g}/\text{mL}$) in the presence of RNAase A (100 $\mu\text{g}/\text{mL}$) for 30 min at 37 °C in the dark. The stained cells were then analyzed using the flow cytometer.

4.9. Apoptosis assay by Hoechst 33342 staining

HeLa cells (3×10^5 cells per well in 6-well plate) were incubated for 24 h and then exposed to different concentrations of **Ru1** or **Ru2** complex for 24 h, respectively. After treatment, cells were stained with 5 $\mu\text{g}/\text{mL}$ Hoechst 33342, washed twice with

PBS, and then photographed using an inverted fluorescence microscope.

4.10. AO/EB staining method

HeLa cells were seeded in 6-well plates and treated in the absence or presence of Ru(II) complexes for 24 h. After incubation, cells were washed twice with ice-cold PBS and stained with 100 $\mu\text{g}/\text{mL}$ concentration of AO/EB solutions, and then photographed using an inverted fluorescence microscope.

4.11. Apoptosis assay by annexin V/PI double staining

Different stages of apoptosis were distinguished using annexin V-FITC Apoptosis Detection Kit. After incubation with various concentrations of complexes for 24 h, cells were harvested and washed twice with PBS, and then resuspended in 500 μL binding buffer. The suspension were stained with 5 μL Annexin V-FITC and 10 μL PI at room temperature for 15 min in the dark, and then analyzed using the flow cytometer.

4.12. Caspase activity assay

According to the manufacturer's protocol, HeLa cells were collected and suspended in cell lysis buffer, and then incubated on ice for 15 min. After centrifugation at 15,000 g for 15 minutes, the supernatants were collected and seeded into 96-well plates. After then, specific caspase substrates, including Ac-DEVD-*p*NA for caspase-3, Ac-IETD-*p*NA for caspase-8, and Ac-LEHD-*p*NA for caspase-9, were added. Plates were incubated at 37°C for 2 h and caspase activity was determined by a Microplate reader. Relative caspase activity was expressed as the percentage of control (as 100%).

4.13. Reactive oxygen species (ROS) assay

ROS level was detected after HeLa cells had been stained with 2,7-Dichlorodihydrofluorescein diacetate (DCFH-DA). For flow cytometry analysis or microplate analysis, collected cells were trypsinized and washed three times with PBS, and then

incubated for 20 min with 10 μ M DCFH-DA in culture medium at 37 °C in the dark. Cells were washed twice and resuspended in PBS, and then analyzed by a flow cytometer or a microplate analyzer. For microscopic observation, cells were incubated for 20 min in complete medium containing 10 μ M DCFH-DA and washed twice with PBS, and then photographed using an inverted fluorescence microscope. When necessary, antioxidants (NAC = 10 mM and GSH = 5 mM) were added in medium for 1 h before addition of Ru(II) complexes.

4.14. MMP measurement

The mitochondrial membrane potential was analyzed using flow cytometry and inverted fluorescence microscope after HeLa cells had been stained with the mitochondrial dye JC-1. Briefly, HeLa cells were placed in 6-well plates at 2×10^5 cells per well with various concentrations of Ru(II) complexes for different times. For flow cytometry analysis, the cells were gently collected and incubated in 500 μ L PBS containing 10 μ g/mL JC-1 for 30 min at 37 °C in the dark. Then cells were re-suspended in PBS and then analyzed by a flow cytometer immediately. For microscopic observation, cells were incubated in complete medium containing 10 μ g/mL JC-1 for 30 min and washed twice with PBS, image of the cells were photographed immediately by an inverted fluorescence microscope.

4.15. Comet assay

DNA damage was detected by single-cell gel electrophoresis as previously described [34]. Single-cell gel electrophoresis was performed using the Comet assay reagent kit purchased from Trevigen according to the manufacturer's instructions. DNA was stained with SYBR Green I (Trevigen) and photographed by an inverted fluorescence microscope.

4.16. Western blotting analysis

For total protein isolation, cells were harvested in lysis buffer containing radio immunoprecipitation assay (RIPA) buffer, phenylmethanesulfonyl fluoride (PMSF)

and phosphatase inhibitors mixture. For cytochrome *c*, the cytosol fraction was isolated from the total cell lysates using Cell Mitochondria Isolation Kit. The protein concentrations were determined by BCA Protein Assay Kit. The effects of **Ru1** on the expression levels of proteins associated with cell cycle relative, DNA damage, Bcl-2 family and caspase were examined by western blot analysis.

4.17. Real-time living cell imaging

HeLa cells were placed into 20 mm class bottom cell culture dish and incubated for 24 h. Then cell mitochondria and nucleuses were stained with 100 nM Mito Tracker Red CMXRos and 2 $\mu\text{g}/\text{mL}$ DAPI for 20 min, respectively. After washing with PBS twice, cells were cultured in fresh medium contained with 4.0 μM of **Ru1** on Tokai hit INUBG2ETFP-WSKM at 37 °C with 5% CO₂. Cell images were captured with inverted fluorescence microscope at different time intervals.

Acknowledgements

This work was supported by the National Natural Science Foundation of China (21701034), the Natural Science Foundation of Guangdong Province (No.S2013010011660), Training Plan of Guangdong Province Outstanding Young Teachers in Higher Education Institutions (No.YQ201401, YQ2015086), the Medical Scientific Research Foundation of Guangdong Province of China (No.A2015500, A2016464, A2017309), and the University Student Innovation Experiment Program (No. 201710571004, 201710571017).

References

- [1] P.C. Bruijninx, P.J. Sadler, New trends for metal complexes with anticancer activity, *Curr. Opin. Chem. Biol.* 12 (2008) 197-206.
- [2] L. Kelland, The resurgence of platinum-based cancer chemotherapy, *Nat. Rev. Cancer* 7 (2007) 573-584.
- [3] S.P. Fricker, Metal based drugs: from serendipity to design, *Dalton Trans.* 43 (2007) 4903-4917.
- [4] C.M. Che, J.S. Huang, Ruthenium and osmium porphyrin carbene complexes: synthesis,

- structure, and connection to the metal-mediated cyclopropanation of alkenes, *Coord. Chem. Rev.* 231 (2002) 151-164.
- [5] K.D. Mjos, C. Orvig, *Metallo drugs in medicinal inorganic chemistry*, *Chem. Rev.* 114 (2014) 4540-4563.
- [6] J. M. Rademaker-Lakhai, D. v. d. Bongard, D. Pluim, J. H. Beijnen, J. H. M. Schellens, A Phase I and Pharmacological Study with Imidazolium-trans-DMSO-imidazole-tetrachlororuthenate, a Novel Ruthenium Anticancer Agent, *Clin. Cancer Res.* 10 (2004) 3717-3727.
- [7] C.G. Hartinger, S. Zorbas-Seifried, M.A. Jakupec, B. Kynast, H. Zorbas, B. K. Keppler, From bench to bedside – preclinical and early clinical development of the anticancer agent indazolium trans-[tetrachlorobis(1H-indazole)ruthenate(III)] (KP1019 or FFC14A), *J. Inorg. Biochem.* 100 (2006) 891-904.
- [8] C.G. Hartinger, M.A. Jakupec, S. Zorbas - Seifried, M. Groessler, A. Egger, W. Berger, H. Zorbas, P.J. Dyson, B.K. Keppler, KP1019, A new redox-active anticancer agent—preclinical development and results of a clinical phase I study in tumor patients, *Chem. Biodivers.* 5 (2008) 2140-2155.
- [9] A. Castonguay, C. Doucet, M. Juhas, D. Maysinger, New ruthenium (II)eletozole complexes as anticancer therapeutics, *J. Med. Chem.* 55 (2012) 8799-8806.
- [10] H.K. Liu, J.A. Parkinson, J. Bella, F.Y. Wang, P.J. Sadler, Penetrative DNA intercalation and G-base selectivity of an organometallic tetrahydroanthracene Ru(II) anticancer complex, *Chem. Sci.* 1 (2010) 258-270.
- [11] R.N. Garner, J.C. Gallucci, K.R. Dunbar, C. Turro, $[\text{Ru}(\text{bpy})_2(5\text{-cyanouracil})_2]^{2+}$ as a potential light-activated dual-action therapeutic agent, *Inorg. Chem.* 50 (2011) 9213-9215.
- [12] R.E. Morris, R.E. Aird, P. del Socorro Murdoch, H. Chen, J. Cummings, N.D. Hughes, S. Parsons, A. Parkin, G. Boyd, D.I. Jodrell, P.J. Sadler, Inhibition of cancer cell growth by ruthenium(II) arene complexes, *J. Med. Chem.* 44 (2001) 3616-3621.
- [13] P. C. A. Bruijninx, P. J. Sadler, Controlling platinum, ruthenium, and osmium reactivity for anticancer drug design, *Adv. Inorg. Chem.* 61 (2009) 1-62.
- [14] C. Scolaro, A. Bergamo, L. Brescacin, R. Delfino, M. Cocchietto, G. Laurency, T.J. Geldbach, G. Sava, P.J. Dyson, In vitro and in vivo evaluation of ruthenium(II)–arene PTA complexes, *J. Med. Chem.* 48 (2005) 4161-4171.
- [15] P.J. Dyson, G. Sava, Metal-based antitumour drugs in the post genomic era, *Dalton Trans.* 16 (2006) 1929-1933.
- [16] H. Huang, P. Zhang, H. Chen, L. Ji and H. Chao, Cyclometalated ruthenium(II) anthraquinone complexes exhibit strong anticancer activity in hypoxic tumor cells, *Chem. Eur. J.* 21 (2015) 15308-15319.
- [17] H. Huang, P. Zhang, B. Yu, Y. Chen, J. Wang, L. Ji, H. Chao, Targeting nucleus DNA with a cyclometalated dipyridophenazineruthenium(II) complex, *J. Med. Chem.* 57 (2014) 8971-8983.

- [18] B. Pena, A. David, C. Pavani, M.S. Baptista, J.P. Pellois, C. Turro, K.R. Dunbar, Cytotoxicity studies of cyclometallated ruthenium(II) compounds: new applications for ruthenium dyes, *Organometallics* 33 (2014) 1100-1103.
- [19] J.P. Djukic, J.B. Sortais, L. Barloy, M. Pfeffer, Cycloruthenated compounds-synthesis and applications, *Eur. J. Inorg. Chem.* 7 (2009) 817-853.
- [20] B.A. Albani, B. Pena, K.R. Dunbar, C. Turro, New cyclometallated Ru(II) complex for potential application in photochemotherapy? *Photochem. Photobiol. Sci.* 13 (2014) 272-280.
- [21] J. Maksimoska, L. Feng, K. Harms, C. Yi, J. Kissil, R. Marmorstein, E. Meggers, Targeting large kinase active site with rigid, bulky octahedral ruthenium complexes, *J. Am. Chem. Soc.* 130 (2008) 15764-15765.
- [22] M.A. Jakupec, M. Galanski, V.B. Arion, C.G. Hartinger, B.K. Keppler, Antitumor metal compounds: more than theme and variations, *Dalton Trans.* 14 (2008) 183-194.
- [23] T. Respondek, R.N. Garner, M.K. Herroon, I. Podgorski, C. Turro, J.J. Kodanko, Light activation of a cysteine protease inhibitor: caging of a peptidomimetic nitrile with Ru^{II}(bpy)₂, *J. Am. Chem. Soc.* 133 (2011) 17164-17167.
- [24] R. Cao, W. Peng, Z. Wang, A. Xu, β -Carboline alkaloids: biochemical and pharmacological functions, *Curr. Med. Chem.* 14 (2007) 479-500.
- [25] H.J. Guan, X.D. Liu, W.L. Peng, R.H. Cao, Y. Ma, H.S. Chen, A.L. Xu, β -carboline derivatives: Novel photosensitizers that intercalate into DNA to cause direct DNA damage in photodynamic therapy, *Biochem. Biophys. Res. Commun.* 342 (2006) 894-901.
- [26] A. Kamal, M. Sathish, V.L. Nayak, V. Srinivasulu, B. Kavitha, Y. Tangella, D. Thummuri, C. Bagul, N. Shankaraiah, N. Nagesh, Design and synthesis of dithiocarbamate linked β -carboline derivatives: DNA topoisomerase II inhibition with DNA binding and apoptosis inducing ability, *Bioorg. Med. Chem.* 23 (2015) 5511-5526.
- [27] A. Kamal, V. Srinivasulu, V.L. Nayak, M. Sathish, N. Shankaraiah, C. Bagul, N.V. Reddy, N. Rangaraj, N. Nagesh, Design and synthesis of C3-pyrazole/chalcone-linked β -carboline hybrids: antitopoisomerase I, DNA-interactive, and apoptosis-inducing anticancer agents, *ChemMedChem* 9 (2014) 2084-2098.
- [28] Y. Chen, M.Y. Qin, J.H. Wu, L. Wang, H. Chao, L.N. Ji, A.L. Xu, Synthesis, characterization, and anticancer activity of ruthenium(II)- β -carboline complex, *Eur. J. Med. Chem.* 70 (2013) 120-129.
- [29] Y. Chen, M.Y. Qin, L. Wang, H. Chao, L.N. Ji, A.L. Xu, A ruthenium(II) β -carboline complex induced p53-mediated apoptosis in cancer cells, *Biochimie*, 95 (2013) 2050-2059.
- [30] C. Tan, S. Lai, S. Wu, S. Hu, L. Zhou, Y. Chen, M. Wang, Y. Zhu, W. Lian, W. Peng, L. Ji, A. Xu, Nuclear permeable ruthenium(II) β -carboline complexes induce autophagy to antagonize mitochondrial-mediated apoptosis, *J. Med. Chem.* 53 (2010) 7613-7624.
- [31] J. Dong, X.X. Shi, J.J. Yan, J. Xing, Q.A. Zhang, S. Xiao, Efficient and Practical One-Pot Conversions of N-Tosyltetrahydroisoquinolines into Isoquinolines and of N-Tosyltetrahydro- β -carbolines into β -Carbolines through Tandem beta-Elimination and

- Aromatization, *Eur. J. Org. Chem.* 2010 (2010) 6987-6992.
- [32] M.L. Muro-Small, J.E. Yarnell, C.E. McCusker, F.N. Castellano, Spectroscopy and photophysics in cyclometalated Ru^{II}-Bis(bipyridyl) complexes, *Eur. J. Inorg. Chem.* 25 (2012) 4004-4011.
- [33] J.K. Barton, A.T. Danishefsky, J.M. Golberg, Tris(phenanthroline)ruthenium(II): stereoselectivity in binding to DNA, *J. Am. Chem. Soc.* 106 (1984) 2172-2176.
- [34] L.M. Chen, F. Peng, G.D. Li, X.M. Jie, K.R. Cai, C. Cai, Y. Zhong, H. Zeng, W. Li, Z. Zhang, J.C. Chen, The studies on the cytotoxicity in vitro, cellular uptake, cell cycle arrest and apoptosis-inducing properties of ruthenium methylimidazole complex [Ru(MeIm)₄(p-cpip)]²⁺, *J. Inorg. Biochem.* 156 (2016) 64-74.
- [35] G.B. Jiang, X. Zheng, J.H. Yao, B.J. Han, W. Li, J. Wang, H.L. Huang, Y.J. Liu, Ruthenium(II) polypyridyl complexes induce BEL-7402 cell apoptosis by ROS-mediated mitochondrial pathway, *J. Inorg. Biochem.* 141 (2014) 170-179.
- [36] J.Q. Wang, P.Y. Zhang, C. Qian, X.J. Hou, L.N. Ji, H. Chao, Mitochondria are the primary target in the induction of apoptosis by chiral ruthenium(II) polypyridyl complexes in cancer cells, *J. Biol. Inorg. Chem.* 19 (2014) 335-348.
- [37] C. Tan, S. Wu, S. Lai, M. Wang, Y. Chen, L. Zhou, Y. Zhu, W. Lian, W. Peng, L. Ji, A. Xu, Synthesis, structures, cellular uptake and apoptosis-inducing properties of highly cytotoxic ruthenium-Norharman complexes, *Dalton Trans.* 40 (2011) 8611-8621.
- [38] M.D. Hall, S. Amjadi, M. Zhang, P.J. Beale, T.W. Hambley, The mechanism of action of platinum(IV) complexes in ovarian cancer cell lines, *J. Inorg. Biochem.* 98 (2004) 1614-1624.
- [39] S.P. Oldfield, M.D. Hall, J.A. Platts, Calculation of lipophilicity of a large, diverse dataset of anticancer platinum complexes and the relation to cellular uptake, *J. Med. Chem.* 50 (2007) 5227-5237.
- [40] A.J. Millett, A. Habtemariam, I. Romero-Canelon, G.J. Clarkson, P.J. Sadler, Contrasting Anticancer Activity of Half-Sandwich Iridium(III) Complexes Bearing Functionally Diverse 2-Phenylpyridine Ligands, *Organometallics* 34 (2015) 2683-2694.
- [41] H. Huang, P. Zhang, H. Chen, L. Ji, H. Chao, Comparison between polypyridyl and cyclometalated ruthenium(II) complexes: anticancer activities against 2D and 3D cancer models, *Chemistry* 21 (2015) 715-725.
- [42] S.H. van Rijt, A. Mukherjee, A.M. Pizarro, P.J. Sadler, Cytotoxicity, hydrophobicity, uptake, and distribution of osmium(II) anticancer complexes in ovarian cancer cells, *J. Med. Chem.* 53 (2010) 840-849.
- [43] S. Nikolic, L. Ranganamy, N. Gligorijevic, S. Arandelovic, S. Radulovic, G. Gasser, S. Grguric-Sipka, Synthesis, characterization and biological evaluation of novel Ru(II)-arene complexes containing intercalating ligands, *J. Inorg. Biochem.* 160 (2016) 156-165.
- [44] U. Schatzschneider, J. Niesel, I. Ott, R. Gust, H. Alborzina, S. Wolf, Cellular uptake, cytotoxicity, and metabolic profiling of human cancer cells treated with ruthenium(II)

- polypyridyl complexes $[\text{Ru}(\text{bpy})_2(\text{N-N})\text{Cl}_2]$ with N-N=bpy, phen, dpq, dppz, and dppn, *ChemMedChem* 3 (2008) 1104-1109.
- [45] R. Cao, J. Jia, X. Ma, M. Zhou, H. Fei, Membrane localized iridium(III) complex induces endoplasmic reticulum stress and mitochondria-mediated apoptosis in human cancer cells, *J. Med. Chem.* 56 (2013) 3636-3644.
- [46] C.A. Puckett, J.K. Barton, Mechanism of cellular uptake of a ruthenium polypyridyl complex, *Biochemistry* 47 (2008) 11711-11716.
- [47] C. Li, M. Yu, Y. Sun, Y. Wu, C. Huang, F. Li, A nonemissive iridium(III) complex that specifically lights-up the nuclei of living cells, *J. Am. Chem. Soc.* 133 (2011) 11231-11239.
- [48] W. Cao, W. Zheng, T. Chen, Ruthenium polypyridyl complex inhibits growth and metastasis of breast cancer cells by suppressing FAK signaling with enhancement of TRAIL-induced apoptosis, *Sci. Rep.* 5 (2015) 9157.
- [49] Z. Zhao, Z. Luo, Q. Wu, W. Zheng, Y. Feng, T. Chen, Mixed-ligand ruthenium polypyridyl complexes as apoptosis inducers in cancer cells, the cellular translocation and the important role of ROS-mediated signaling, *Dalton Trans.* 43 (2014) 17017-1702.
- [50] W. Guo, W. Zheng, Q. Luo, X. Li, Y. Zhao, S. Xiong, F. Wang, Transferrin serves as a mediator to deliver organometallic ruthenium (II) anticancer complexes into cells, *Inorg. Chem.* 52 (2013) 5328-5338.
- [51] S. Chatterjee, S. Kundu, A. Bhattacharyya, C.G. Hartinger, P.J. Dyson, The ruthenium(II)-arene compound RAPTA-C induces apoptosis in EAC cells through mitochondrial and p53-JNK pathways, *J. Biol. Inorg. Chem.* 13 (2008) 1149-1155
- [52] C. Wang, Z. Li, M. Fu, T. Bouras, R.G. Pestell, Signal transduction mediated by cyclin D1: from mitogens to cell proliferation: a molecular target with therapeutic potential, in: *Molecular Targeting and Signal Transduction*, Springer, 2004, 217-237.
- [53] T. Abbas, A. Dutta, p21 in cancer: intricate networks and multiple activities, *Nature Reviews Cancer* 9 (2009) 400-414.
- [54] D.O. Morgan, *The cell cycle: principles of control*, New Science Press, 2007.
- [55] K.H. Vousden, X. Lu, Live or let die: the cell's response to p53, *Nature Reviews Cancer* 2 (2002) 594-604.
- [56] M. Malumbres, M. Barbacid, Cell cycle, CDKs and cancer: a changing paradigm, *Nature Reviews Cancer* 9 (2009) 153-166.
- [57] L. Cattaruzza, D. Fregona, M. Mongiat, L. Ronconi, A. Fassina, A. Colombatti, D. Aldinucci, Antitumor activity of gold(III)-dithiocarbamate derivatives on prostate cancer cells and xenografts, *Int. J. Cancer* 128 (2011) 206-215.
- [58] P.R. Florindo, D.M. Pereira, P.M. Borralho, C.M. Rodrigues, M.F. Piedade, A.C. Fernandes, Cyclopentadienyl-ruthenium(II) and iron(II) organometallic compounds with carbohydrate derivative ligands as good colorectal anticancer agents, *J. Med. Chem.* 58 (2015) 4339-4347.
- [59] Q.P. Qin, Z.F. Chen, J.L. Qin, X.J. He, Y.L. Li, Y.C. Liu, K.B. Huang, H. Liang, Studies on antitumor mechanism of two planar platinum(II) complexes with 8-hydroxyquinoline:

- synthesis, characterization, cytotoxicity, cell cycle and apoptosis, *Eur. J. Med. Chem.* 92 (2015) 302-313.
- [60] H. Lai, Z. Zhao, L. Li, W. Zheng, T. Chen, Antiangiogenic ruthenium(II) benzimidazole complexes, structure-based activation of distinct signaling pathways, *Metallomics* 7 (2015) 439-447.
- [61] A. Takahashi, E.S. Alnemri, Y.A. Lazebnik, T. Fernandes-Alnemri, G. Litwack, R.D. Moir, R.D. Goldman, G.G. Poirier, S.H. Kaufmann, W.C. Earnshaw, Cleavage of lamin A by Mch2 alpha but not CPP32: multiple interleukin 1 beta-converting enzyme-related proteases with distinct substrate recognition properties are active in apoptosis, *Proc. Natl. Acad. Sci. USA* 93 (1996) 8395-8400.
- [62] K. Wang, X.Y. Fu, X.T. Fu, Y.J. Hou, J. Fang, S. Zhang, M.F. Yang, D.W. Li, L.L. Mao, J.Y. Sun, H. Yuan, X.Y. Yang, C.D. Fan, Z.Y. Zhang, B.L. Sun, DSePA Antagonizes High Glucose-Induced Neurotoxicity: Evidences for DNA Damage-Mediated p53 Phosphorylation and MAPKs and AKT Pathways, *Mol. Neurobiol.* 53 (2016) 4363-4374.
- [63] T. Ozben, Oxidative stress and apoptosis: impact on cancer therapy, *J. Pharm. Sci.* 96 (2007) 2181-2196.
- [64] H.U. Simon, A. Haj-Yehia, F. Levi-Schaffer, Role of reactive oxygen species (ROS) in apoptosis induction, *Apoptosis* 5 (2000) 415-418.
- [65] C. Fan, J. Chen, Y. Wang, Y.-S. Wong, Y. Zhang, W. Zheng, W. Cao, T. Chen, Selenocystine potentiates cancer cell apoptosis induced by 5-fluorouracil by triggering reactive oxygen species-mediated DNA damage and inactivation of the ERK pathway, *Free Radic. Biol. Med.* 65 (2013) 305-316.
- [66] P.Kumar, S. Dasari, A.K. Patra, Ruthenium(II) complexes of saccharin with dipyrroquinoxaline and dipyrrophenazine: Structures, biological interactions and photoinduced DNA damage activity, *Eur. J. Med. Chem.* 136 (2017) 52-62.
- [67] J. Chen, G. Li, F. Peng, X. Jie, G. Dongye, Y. Zhong, R. Feng, B. Li, J. Qu, Y. Ding, L. Chen, Investigation of inducing apoptosis in human lung cancer A549 cells and related mechanism of a ruthenium(II) polypyridyl complex, *Inorg. Chem. Commun.* 69 (2016) 35-39.
- [68] W.P. Roos, B. Kaina, DNA damage-induced cell death by apoptosis, *Trends Mol. Med.* 12 (2006) 440-450.
- [69] V. Romanov, T.C. Whyard, W.C. Waltzer, A.P. Grollman, T. Rosenquist, Aristolochic acid-induced apoptosis and G2 cell cycle arrest depends on ROS generation and MAP kinases activation, *Arch. Toxicol.* 89 (2015) 47-56.
- [70] S.W. Lee, M.H. Lee, J.H. Park, S.H. Kang, H.M. Yoo, S.H. Ka, Y.M. Oh, Y.J. Jeon, C.H. Chung, SUMOylation of hnRNP - K is required for p53 - mediated cell - cycle arrest in response to DNA damage, *EMBO J.* 31 (2012) 4441-4452.
- [71] B.P. Sullivan, D.J. Salmon, T.J. Meyer, Mixed Phosphine 2,2'-Bipyridine Complexes of Ruthenium, *Inorg. Chem.* 17 (1978) 3334-3341.
- [72] L.Chen, G. Li, F. Peng, X. Jie, G. Dongye, K. Cai, R. Feng, B. Li, Q. Zeng, K. Lun, J. Chen,

B.Xu, The induction of autophagy against mitochondria-mediated apoptosis in lung cancer cells by a ruthenium (II) imidazole complex, *Oncotarget* 7 (2016) 80716-80734.

ACCEPTED MANUSCRIPT

Research highlights

- Two new cyclometalated Ru(II) complexes were synthesized and characterized.
- **Ru1** and **Ru2** against four cancer cells and one normal cell was evaluated.
- **Ru1** and **Ru2** mainly accumulated in the nuclei in HeLa cancer cells.
- The cellular uptake and apoptosis-inducing mechanism were explored.
- The mitochondrial membrane potential, ROS and DNA damage were investigated.